PFC/RR-83-22 DOE/ET/51013-93

SLOSHING-ION EQUILIBRIA IN THE TARA ENDPLUGS

S. Hokin, J. Kesner

Plasma Fusion Center
Massachusetts Institute of Technology
Cambridge, MA 02139

November 1983

This work was supported by the U. S. Department of Energy Contract No. DE-AC02-78ET51013. Reproduction, translation, publication, use and disposal, in whole or in part by or for the United States government is permitted.

ABSTRACT

We have employed a modified version of the LLNL Bounce-average Fokker-Planck code[1] to model neutral beam-produced sloshing-ion equilibria in the TARA endplugs. The questions we have addressed concern the effect of deuterium beam operation as opposed to hydrogen operation, and the advantage of using full-energy beams rather than the usual three-component beams. We find that, for the expected "base case" TARA operating parameters, a 40% savings in required beam power is attained by using deuterium beams rather than hydrogen beams, and that the use of full-energy beams results in an additional 26% power savings for these parameters. For higher plasma temperatures the use of full-energy beams becomes significantly advantagous. We have also investigated the equilibria of two possible alternate mirror configurations for the TARA endplugs, believed to be more stable to trapped particle modes, and report those results here.

INTRODUCTION

It has been conjectured that converting the TARA endplug neutral beams from hydrogen operation to deuterium operation at comparable energy could have some beneficial effects. These are that (a) the deuterium beam would be better absorbed due to the larger cross-sections that result from the lower particle speed, and (b) that the charge-exchange pumping of cold ions trapped in the thermal barrier would be enhanced due to the larger ratio of σ_{cx}/σ_i for deuterium. This second point seems to imply that a larger thermal barrier potential drop might be obtained with deuterium.

Another possible modification of the beam is the elimination of the one-half- and one-third-energy components that normally compose over half of a neutral beam's current. The advantages of an all-full-energy neutral beam in the TARA endplugs would be (a) an increased plasma fueling efficiency due to a smaller ratio of σ_{cx}/σ_i, and (b) less interaction between the plasma potential and the beam ions (the one-third-energy component of a 20 keV H beam is comparable in energy to a predicted 2 keV midplane-to-peak potential rise). The disadvantages of an all-full-energy beam are a reduction in absorption efficiency due to the decreased total cross-section, and a relative decrease in charge-exchange pumping due to the decreased σ_{cx}/σ_i.

Some alternate mirror and beam injection configurations have been envisioned for the TARA endplugs with the hope of making them more stable to trapped particle modes; these are (a) 40 degree midplane injection into a symmetric mirror with a lower mirror ratio than that given in the TARA proposal, and (b) perpendicular injection into an asymmetric mirror with a low mirror ratio whose field minimum is located in the outside half of the plug. These alternative configurations have a lower β in the bad curvature region of the plug and are hoped to provide less driving force to possible trapped particle instability. To be useful, they must provide adequate confinement of the fast ions.

Clearly there are competing factors here, and a more detailed calculation is needed. We have employed a modified version of the LLNL Bounce-Average Fokker-Planck code [1], which models a beam-injected mirror by evaluating and bounce-averaging the collision operator along a field line and evolving the midplane ion distribution function using a finite element method. In the next section we will discuss our choice of parameters, and in section 3 we will present our results and some concluding remarks.

CHOICE OF ENDPLUG PARAMETERS

We will attempt to model 40 degree neutral beam injection into an R=6 plug, 93 cm. in length from midplane to throat, where R is the mirror ratio; the magnetic field is modeled to be parabolic in z, where z is the axial distance from the midplane. Neutral beam parameters have been chosen to be consistent with the numbers presented in the TARA proposal,[2] and are listed in Table 1. The following describes our selection of plasma parameters for the plug.

Figure 1 shows a potential profile for a tandem mirror with a thermal barrier. The code models half of a simple mirror, and thus only models half of the endplug between the point b and point t. The relation between the central cell density, n_c, thermal barrier potential drop, $\delta\phi_b$, central cell temperature, T_c (assumed to be equal for electrons and ions), midplane density n(b), and fraction of cold ($T=T_c$) electrons in the plug, f_{ec}, is:

$$f_{ec}n(b) = n_c e^{-\delta\phi_b/T_c} \qquad (1)$$

Choosing $n(b)=5.0 \times 10^{12}\ cm^{-3}$, $n_c=1.0 \times 10^{13}\ cm^{-3}$, and $f_{ec}=0.1$ results in a value of $\delta\phi_b=3T_c$. To effectively plug the central cell ions, one hopes that

the plugging potential, $\delta\phi_c$, would be about $2T_c$. Thus, the midplane-to-peak potential rise, $\delta\phi_a$, is desired to be about $5T_c$.

The endplug is heated by ECRH to produce a "hot" electron population at a temperature of many keV responsible for the existence of the thermal barrier, and a "warm" electron population at $T=T_{ew}$; in addition, a small fraction (f_{ec}) of "cold" central-cell electrons are present in the plug. It is expected, then, that the potential will peak higher than a simple Boltzmann factor would predict for only warm electrons in the plug, due to the presence of the hot electrons. Cohen et. al.[3] claim that to a good approximation $\delta\phi_a$ satisfies

$$\delta\phi_a = T_{ew} \ell n \left[\frac{n(a)}{f_{ec} n(b)} \sqrt{\frac{T_c}{T_{ew}}} \right] \qquad (2)$$

where n(a) is the peak density at z=a, determined by the code to be 3n(b). Remembering our choices of f_{ec} and $\delta\phi_a$, this equality is satisfied if $T_{ew}/T_c = 1.6$. It is essential to know T_{ew} because it determines the electron-impact ionization cross-section, and is the electron temperature used by the code.

Beyond the endplug there is a transition region which maps the axisymmetric flux surfaces in the endplug to the MHD-stable quadrupole anchor. It is assumed that the potential difference between the plug midplane (z=b) and the throat (z=t), $\delta\phi_{bt}$, is about $2T_c$. Also, the density does not drop to zero at the mirror throat, but is assumed to remain at about $2 \times 10^{13} cm^{-3}$. To accommodate for these effects, and the fact that the potential does not follow a simple Boltzmann relation, we have added a small amount of density to the sloshing-ion profile at the mirror throat to make n(t) as chosen, and we have used a modified Boltzmann relation for the potential,

$$\phi(z) - \phi(b) = C_1 T_{ew} \ell n \left(\frac{n(z) + n_f(z)}{n(b)} \right) \tag{3}$$

where

$$n_f(z) = 0 \qquad (b \leq z \leq a)$$

$$= n_f(t) \frac{\phi(z) - \phi(a)}{\phi(t) - \phi(a)} \qquad (a < z \leq t)$$

and $n_f(t)$ is chosen so that

$$\phi(t) - \phi(b) = C_1 T_{ew} \ell n \left(\frac{n(t) + n_f(t)}{n(b)} \right).$$

For Eqn. (3) to be consistent with eqn. (2) when z=a requires that

$$C_1 = 1 + \ell n \left(\frac{1}{f_{ec}} \sqrt{\frac{T_c}{T_{ew}}} \right) / \ell n \left(\frac{n(a)}{n(b)} \right). \tag{4}$$

C_1 is chosen to be consistent with the code's determination of n(a)/n(b). These modifications make the calculated potential a smooth function of z, and insure that it has the desired value at z=b and z=t. The addition of transition density near the mirror throat is a necessary modification, since without it the potential drop in the outer portion of the plug would be unrealistically large (the sloshing-ion density becomes very small at the mirror throat). Since the minimum energy of a confined fast ion is given by

$$E_{min} = \frac{\delta\phi_{at}}{R/R_{beam} - 1} \tag{5}$$

where $R_{beam} \equiv B_t/B_a$ is the mirror ratio of the peak field to the field at the injection angle bounce point, one can see that the addition of ion density at z=t, and the resulting decrease in $\delta\phi_{at}$, provides much improved beam confinement. Some have compared the transition region to a voltage

divider, separating the potential drop from $\phi=\phi(a)$ to ground potential into two steps, one at the plug throat and the other at the end of the machine. Although we have chosen our parameters so that $\delta\phi_a=5T_c$, $\delta\phi_a$ remains free to vary as a function of n(a)/n(b) (both in the Boltzmann logarithm and the C_1 factor).

We have also taken into account the cold central cell ions, assumed to be Maxwellian, which pass into the endplug. These ions can collisionally scatter and be trapped in the plug and therefore set a non-zero boundary condition on the distribution function in the trapped region of velocity space.[1] The added ion distribution is cut off below an energy $\delta\phi_b$ (the ions pick up this energy as they drop into the potential well) and has a density

$$n_c(b) = \frac{n_c}{R}\sqrt{\frac{T_c}{\pi\delta\phi_b}} \tag{6}$$

which is an approximate relation which comes from an assumption of flux conservation between the central cell and endplug.[4]

A third and very important ion species is not taken into account in the code; these are the ions produced by charge exchange of cold neutral gas which are trapped in the potential well of the thermal barrier. Because of this, the enhanced charge-exchange pumping effect of the D beam will not be fully realized in the results quoted here. The electrons are assumed to be isotropic and Maxwellian throughout the plug, which is certainly not true in the actual machine; however, the sloshing-ion distribution should evolve to an equilibrium state which is fairly insensitive to the details of the electron distribution function as long as the electron distribution has a mean energy of around 3/2 T_{ew}.

To be able to determine beam current requirements from the code's results, we must know the fraction of the beam that is absorbed by the plasma. We choose a parabolic radial density profile

$$n(r) = n_0[1 - (r/a)^2] \tag{7}$$

The absorption decrement of the beam is given by

$$D(s) = \int_0^s ds' n(s') \sigma_{tot} \tag{8}$$

where s is the distance along the beam path. With the beam injected at an angle θ_0 to the plug axis this becomes

$$D(u) = \frac{\sigma_{tot} n_0}{\sin\theta_0} a \int_{-1}^{u} du'[1 - u'^2] \tag{9}$$

where u=r/a and -1<u<1. This gives the total absorption decrement

$$D(u=1) = \frac{4}{3} a \frac{n_0 \sigma_{tot}}{\sin\theta_0} \tag{10}$$

The density n_o must be the average axial density that the beam, which extends over a third of the axial length of the plug, "sees"; this density has been chosen by calculating a beam-profile average of the z-dependent density using a Gaussian profile for the beam intensity (as the code does) and a linear z-dependence of n(z) between z=b and z=a (the beam does not extend beyond z=a). This results in the choice of $n_0 = 1 \times 10^{13}$ cm^{-3}. The plasma radius, a, is chosen to be 7.5 cm. (the factor of 4/3 is twice the profile-weighted radius of the plasma, 2/3 a).

The fraction of the beam absorbed by the plasma, f_{abs}, is

$$f_{abs} = 1 - e^{-D(1)} \tag{11}$$

The total beam current is then calculated from the code's result for the field-line integral of the source using the relation

$$I_{beam} = \frac{(\text{line current})}{f_{abs}} \pi \left(\frac{2}{3} a\right)^2 1.6 \times 10^{-19} \times 2 \times 2 \qquad (12)$$

where the radial density profile-weighted radius has been used to represent the average cross-sectional area of the plasma. The first factor of two accounts for the fact that the code only models half of the plug; the second factor of two is a fudge factor which accounts for a supposed half of the beam ions being lost by charge-exchange on cold neutral gas. The required beam current calculated here is only a rough estimate; however, the comparison between results for different cases should be fairly accurate.

RESULTS

We have chosen T_c=400eV for the TARA base case parameters, making T_{ew}=640eV. We are informed by the neutral beam experts[5] that a 20 keV H beam can be converted to a D beam with minimal changes in the source geometry if the D beam is run at 25 keV; these are the beam energies used in the calculation. The beams are chosen to have three energy components with current fractions in the ratio of 3:2:3, which corresponds to 60% monatomic ions, 20% diatomic ions, and 20% triatomic ions in the neutral beam plasma source. Table 1 describes the neutral beam sources assumed here.

Columns (a) and (b) of table 2 summarize the code's results for a three-component hydrogen beam equilibrium and a three-component deuterium beam equilibrium for the TARA base case parameters. The calculated sloshing-ion density and potential profiles for case (b) are shown in figure 2 (those for case (a) are similar); the midplane ion distribution functions $f(v,\theta,z=0)$ and $f(v_\perp,v_{||},z=0)$ are presented in figures 3 and 4, respectively.

The results for these two cases indicate that n(a)/n(b) is increased slightly for the D case, in spite of the fact that cold trapped ions were absent in the calculation, but in this case it is too little an effect to alter the potential rise $\delta\phi_a$ significantly. However, there is a considerable savings in beam power (43%) due to the lower current needed to sustain equilibrium with a D source. This is due in part to the better confinement of the D beam ($n\tau$ is twice as large) and due in part to the better absorption of the D beam (20% vs. 16% for H).

Column (c) of Table 2 presents the results for a full-energy D beam injected into the plug with the same parameters. Because the full-energy beam is much less effected by the plasma potential than is the three-component beam, its confinement is improved by over a factor of two. This combined with the better fueling efficiency of the full-energy beam is enough of an effect to outweigh the poorer absorption of the beam to result in a further savings of 26% in beam power over the three-component beam case.

As the central cell temperature is raised, the potential needed to plug the central cell ions must also be increased. However, the beams will likely be run at a fixed energy (25 keV for D operation). One then wants to know how large $\delta\phi_a$ can be before the confinement of the beam is degraded to the point where the desired plug equilibrium is no longer attainable with the available power. Because a full-energy beam is less affected by the potential, it will be able to fuel the endplug at larger values of $\delta\phi_a$ than would a three-component beam for a given beam power. We have investigated this effect by computing endplug equilibria for T_c=1000 eV and T_c=2000 eV cases.

Columns (a) and (b) of table 3 present our results for the T_c=1000 eV case with a three-component beam and a full-energy beam, respectively. One sees that the confinement of the full-energy beam is actually increased over the T_c=400 eV case, due to the larger electron-ion collision time at the higher electron temperature (1600 eV). This is outweighed, however, by the

poorer absorption of the beam and the lower fueling efficiency due to the increased value of σ_{cx}/σ_i; the end result is that essentially the same beam power is required by the full-energy beam at T_c=1000eV as was required at T_c =400eV. However, the power requirement of the three-component beam has more than doubled: $n\tau$ has decreased, and the required current has increased due to the larger value of σ_{cx}/σ_i. Where in the T_c=400eV case one gained a 26% decrease in required beam power by switching from a three-component to a full-energy beam, in the T_c=1000eV case a 66% power decrease is found.

Note, also, that in the T_c=1000eV case the average energy of the sloshing ions is actually greater than the injection energy! This can be explained by noting that a large portion of the beam is ionized at a potential larger than that of the midplane, and that ions scattered to lower energy are more poorly confined than ions scattered to higher energy, resulting in a surplus of high energy ions.

Column (c) of Table 3 presents the results for full-energy beam injection with T_c=2000eV. Now the required beam power is considerably increased over the T_c=1000eV case due to degraded confinement of the beam. A three-component beam (not shown) has a confinement time of less than one-sixth that of the full-energy beam for these plasma parameters, and requires an enormous amount of power (over 5 MW) to maintain a highly non-thermalized ion distribution.

We have also computed deuterium three-component beam equilibria for an R=4 parabolic well with 40 degree injection and for an asymmetric R=2 well with perpendicular injection. These results are listed in table 4, and the magnetic field profile for the second case is shown in figure 5. These configurations have been chosen because they have a lower β in the bad curvature region of the plug and are hoped to be more stable to trapped particle modes than were the previous cases.

We found that the R=4 case requires a fairly narrow angle spread of the source, 4 degrees or so, for good confinement since the beam is injected at

an angle close to the loss cone angle of 30 degrees. However, it is believed that such an angle spread of the source is achievable in the experiment; given that, the confinement of the beam is good, with an $n\tau$ of over half that of the R=6 case. The R=4 case produces a sloshing-ion profile which is similar to the R=6 case, although peaked further away from the midplane. Note that the beam current and power requirement quoted are quite high. This is due to the fact that the density is more peaked away from the midplane in the R=4 case than in the R=6 case, due to the smaller angle spread of the source used and the lower mirror ratio, resulting in a line-integrated density which is twice as large for the same midplane density. This means that to have a midplane density of 5×10^{12} cm^{-3}, which is necessary for adequate beam absorption, we must put twice as many ions into the plug. The increase in required power may outweigh the advantages of an R=4 mirror.

The perpendicular injection case has quite good confinement, with an $n\tau$ of close to twice that of the R=6, 40 degree injection case, but exhibits no sloshing-ion peak. The density and potential profiles for this configuration are shown in figure 6; one sees a fairly flat density peak at the field minimum (we have modeled the outer portion of the mirror, and have used a virtual source at the bounce point of the actual source, as indicated in figure 5). Also note that the transition density plays a very strong role in this case, since the fast ion density falls to a low value in the outer third of the modeled region. Because it is unlikely that the enhanced potential provided by a thermal barrier could be achieved for this case, since the density peak coincides with the field minimum, we have set C_1=1. For comparative purposes we chose to keep T_{ew}=640 eV, and to require a midplane-to-throat potential drop of $3T_c$. Without a thermal barrier elevated electron temperatures may not be possible in the plug, which may limit the allowable central cell temperature due to the smaller confining potential. In addition, lower electron temperatures in the plug will provide slightly poorer confinement of the beam, due to increased collisionality, but this is a relatively small effect.

In summary, we conclude that a considerable savings in beam power (40%) is achieved by the use of 25 keV deuterium neutral beams rather than 20 keV hydrogen neutral beams in the TARA endplug for the envisioned plasma parameters. A conversion from three-component beams to full-energy beams produces a 25% savings in required power at these temperatures, which may not justify the added cost of such a conversion. If, however, 1 keV central cell temperatures are attained, the use of full-energy beams becomes significantly advantageous; for higher plasma temperatures the use of full-energy beams is a necessity. Two possible alternative field configurations which are hoped to be more stable to trapped particle modes provide adequate confinement of the beam ions, although one of them may require a substantially larger beam power, and the other may impose an undesirable temperature limit on the central cell.

REFERENCES

[1] Cutler, T.A., Pearlstein, L.D., Rensink, M.E., LLNL Rept. UCRL-52233 (1977); see also Cutler, T.A., "User Guide for the Bounce Average Code", an on-line MFECC document in the file space of user 3040.

[2] Kesner, J., Post, R.S., McVey, B.D., Smith, D.K., Nuclear Fusion 22, 549 (1982).

[3] Cohen, R. H., Berstein, J. B., Dorning, J. J., Roulands, G., LLNL Rept. UCRL-84147 (1980).

[4] Baldwin, D.E., Logan, B.G., Simonen, T.C., LLNL Report UCID-18496-Part 2, pg. IV-84, (1980).

[5] Blackfield, D., private communication of results soon to be published in an MIT report.

TABLE 1
Neutral Beam Source Parameters

Beam Energy:	D injection	25 keV
	H injection	20 keV
Energy spread, $\Delta E/E$:		8%
Current fractions:	Full energy component	37.5%
	Half energy component	25%
	One-third energy component	37.5%
Angle spread (half-angle to 1/e)		9^{o}
Beam width (half-width to 1/e)		28 cm.
Injection Angle		40^{o}

TABLE 2

Code Results, T_c = 400 eV

(TARA base case).

	(a)	(b)	(c)
Fixed Parameters:			
Beam Type	3 component H	3 component D	1 component D
R	6	6	6
T_c (eV)	400	400	400
T_{ew} (eV)	640	640	640
$\delta\phi_b$ (keV)	1.2	1.2	1.2
$\delta\phi_{bt}$ (keV)	0.8	0.8	0.8
n_c (cm^{-3})	1×10^{13}	1×10^{13}	1×10^{13}
n(b) (cm^{-3})	5×10^{12}	5×10^{12}	5×10^{12}
n(t) (cm^{-3})	2×10^{12}	2×10^{12}	2×10^{12}
$\langle E_{inj} \rangle$ (keV)	12.5	15.6	25.0
σ_{cx}/σ_i	3.6	4.2	3.6
beam absorption	16%	20%	16%
Code Results:			
C_1	2.9	2.8	2.7
$\langle E_{ions} \rangle$ (keV)	11.7	14.8	22.2
$\delta\phi_a$ (keV)	2.0	2.1	2.1
n(a) (cm^{-3})	1.5×10^{13}	1.5×10^{13}	1.6×10^{13}
line current ($cm^{-2}s^{-1}$)	3.4×10^{17}	2.0×10^{17}	8.4×10^{16}
line-av. $n\tau$ ($cm^{-3}s$)	1.5×10^{11}	2.9×10^{11}	6.6×10^{11}
midplane $\beta_\perp$, $\beta_{\|\|}$	3.3%, 12%	4.1%, 14%	6.6%, 22%
est. beam current (A)	110	50	23
est. beam power (kW)	1370	780	570

TABLE 3

Code Results, T_c = 1000, 2000 eV

	(a)	(b)	(c)
Fixed Parameters:			
Beam type	3 component D	1 component D	1 component D
R	6	6	6
T_c (eV)	1000	1000	2000
T_{ew} (eV)	1600	1600	3200
$\delta\phi_b$ (eV)	3000	3000	6000
$\delta\phi_{bt}$ (eV)	2000	2000	4000
n_c (cm^{-3})	1×10^{13}	1×10^{13}	1×10^{13}
n(b)	5×10^{12}	5×10^{12}	5×10^{12}
n(t)	2×10^{12}	2×10^{12}	2×10^{12}
$\langle E_{inj} \rangle$ (keV)	15.6	25	25
σ_{cx}/σ_i	5.6	4.5	5.2
beam absorption	20%	15%	15%
Code Results:			
C_1	3.1	2.9	3.1
$\langle E_{ions} \rangle$ (keV)	16.9	25.8	28.7
$\delta\phi_a$ (keV)	4.9	5.1	9.7
n(a)(cm^{-3})	1.3×10^{13}	1.5×10^{13}	1.4×10^{13}
line current ($cm^{-2}s^{-1}$)	4.0×10^{17}	7.1×10^{16}	1.4×10^{17}
line-av. $n\tau$ ($cm^{-3}s$)	2.2×10^{11}	8.9×10^{11}	6.0×10^{11}
midplane $\beta_\perp$, $\beta_{\|\|}$	4.6%, 18%	7.4%, 26%	7.8%, 31%
est. beam current (A)	110	24	46
est. beam power (kW)	1720	590	1160

TABLE 4

Code Results, T_c = 400 eV, Alternate Configurations

	(a)	(b)
Fixed Parameters:		
Beam Type	3 component D* (40° inj.)	3 component D ($\perp$ inj.)
R	4	2.2
T_c(eV)	400	not used
T_{ew}(eV)	640	640
$\delta\phi_b$(eV)	1200	0 (no barrier)
$\delta\phi_{bt}$(eV)	800	$\delta\phi_c$ = 1200
n(b)(cm^{-3})	5×10^{12}	5×10^{12}
n(t)(cm^{-3})	2×10^{12}	2×10^{12}
$\langle E_{inj} \rangle$	15.6	15.6
Code Results:		
C_1	2.7	1.0 (fixed)
$\langle E_{ions} \rangle$(keV)	15.1	12.2
$\delta\phi_a$(keV)	2.2	---
n(a)(cm^{-3})	1.7×10^{13}	---
line current ($cm^{-2} s^{-1}$)	7.4×10^{17}	3.1×10^{16}
line av. $n\tau$ ($cm^{-3} s$)	1.8×10^{11}	5.5×10^{11}
midplane $\beta_\perp$, $\beta_{\parallel}$	2.3%, 7.5%	4.5%, 1.6%
est. beam current (A)	130	55
est. power (kW)	2000	860

*Source has a smaller $\Delta\theta$ spread than in the previous cases.

FIGURE 1

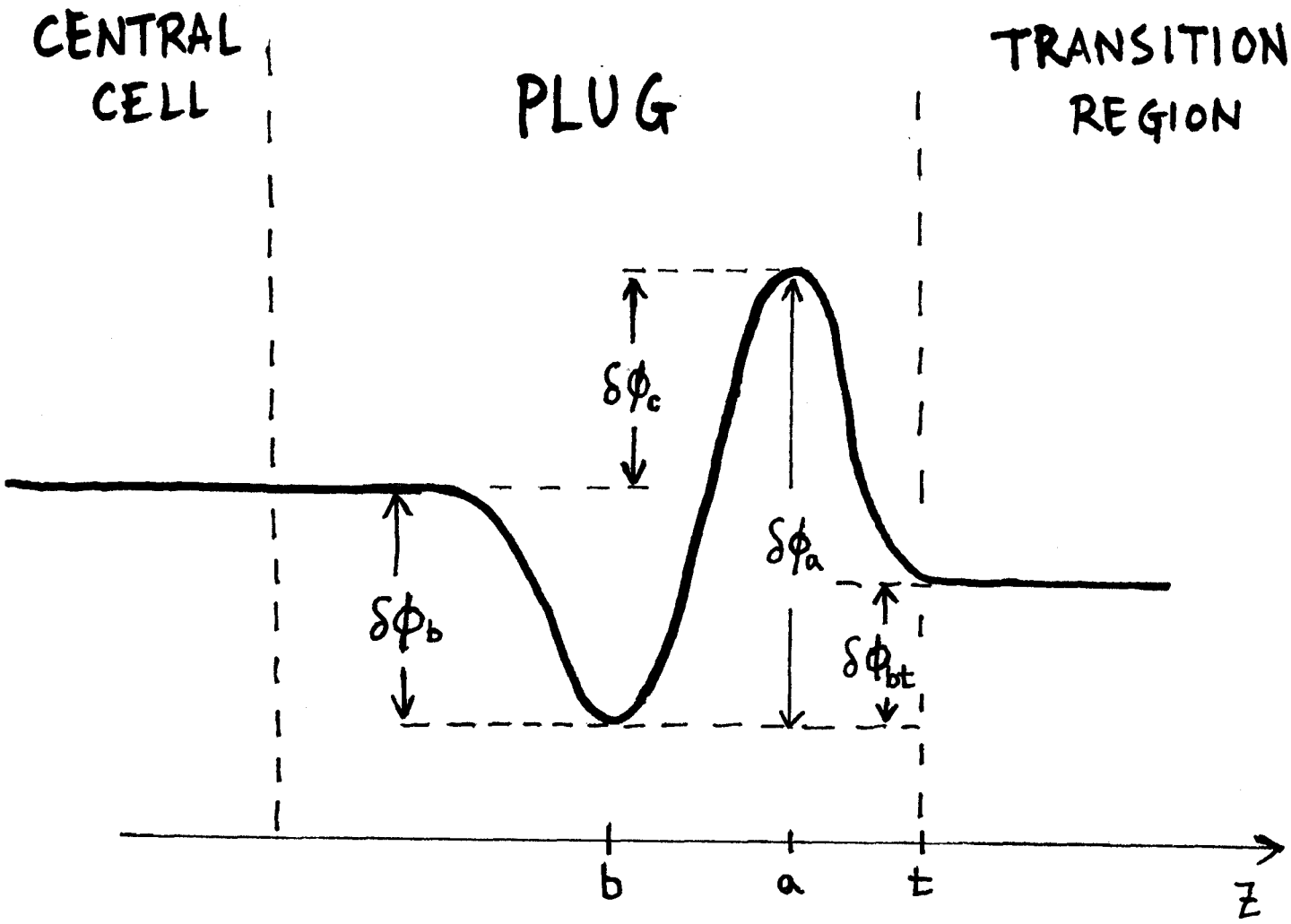

Figure 1: The expected potential profile for a tandem mirror with thermal barrier operation. $\delta\phi_c$ is the central cell ion confining potential and $\delta\phi_b$ is the thermal barrier potential.

FIGURE 2

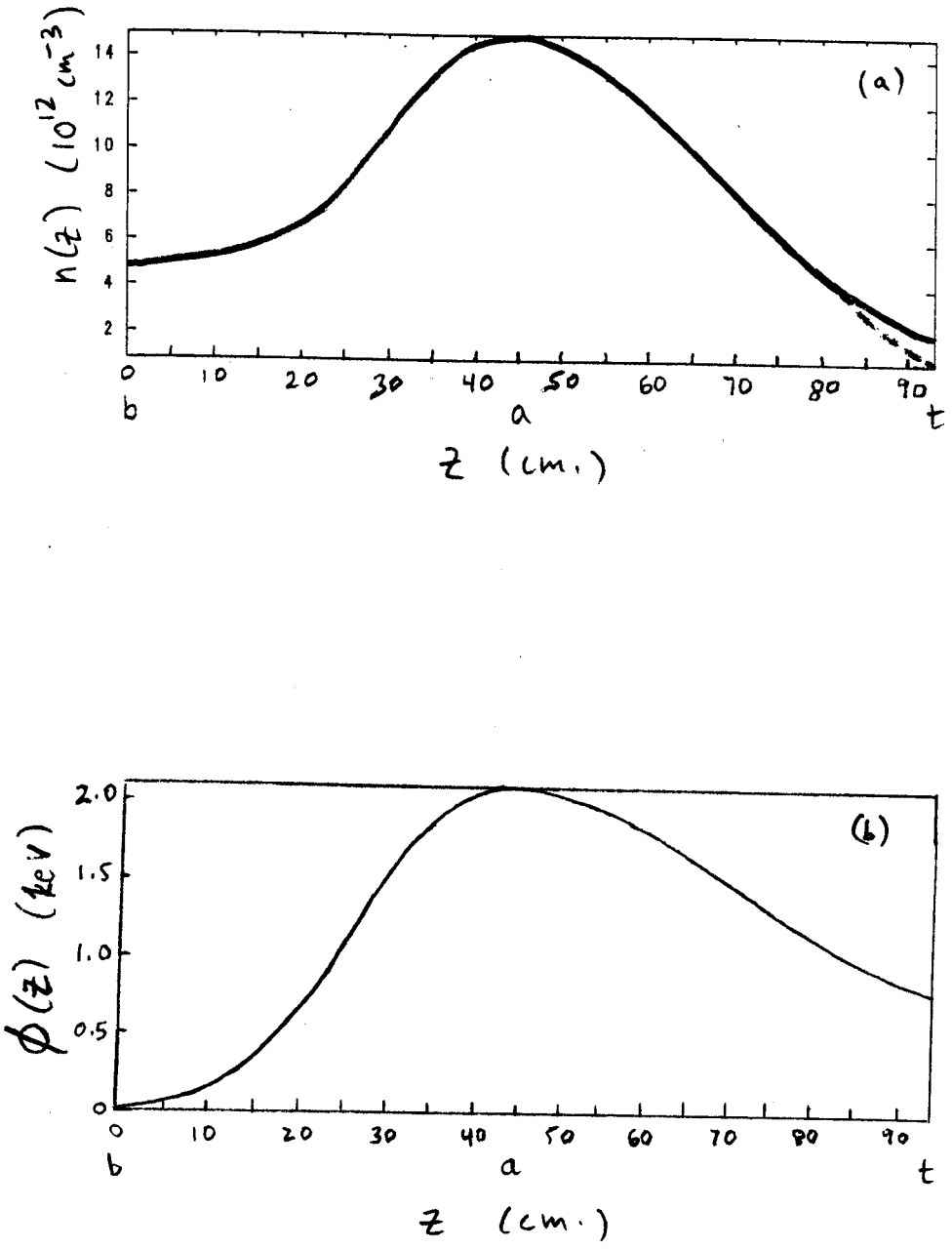

Figure 2: (a) The calculated density profile between the plug midplane and throat for the case presented in column (b) of table 2. The dotted line shows only the sloshing-ion density, whereas the solid line includes transition density.

(b) The resulting potential profile. The throat potential is a fixed boundary condition.

FIGURE 3

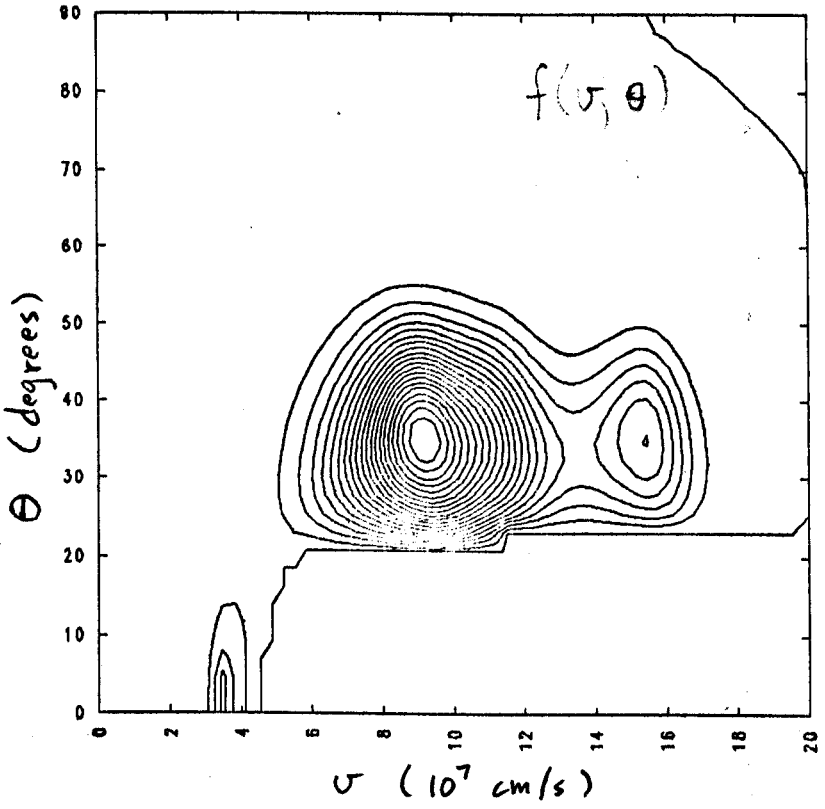

Figure 3: f(v, θ) at the midplane for the ions. The central cell passing ions appear in the lower left hand region. Note that the one-half and one-third energy components of the beam have relaxed into a single peak.

FIGURE 4

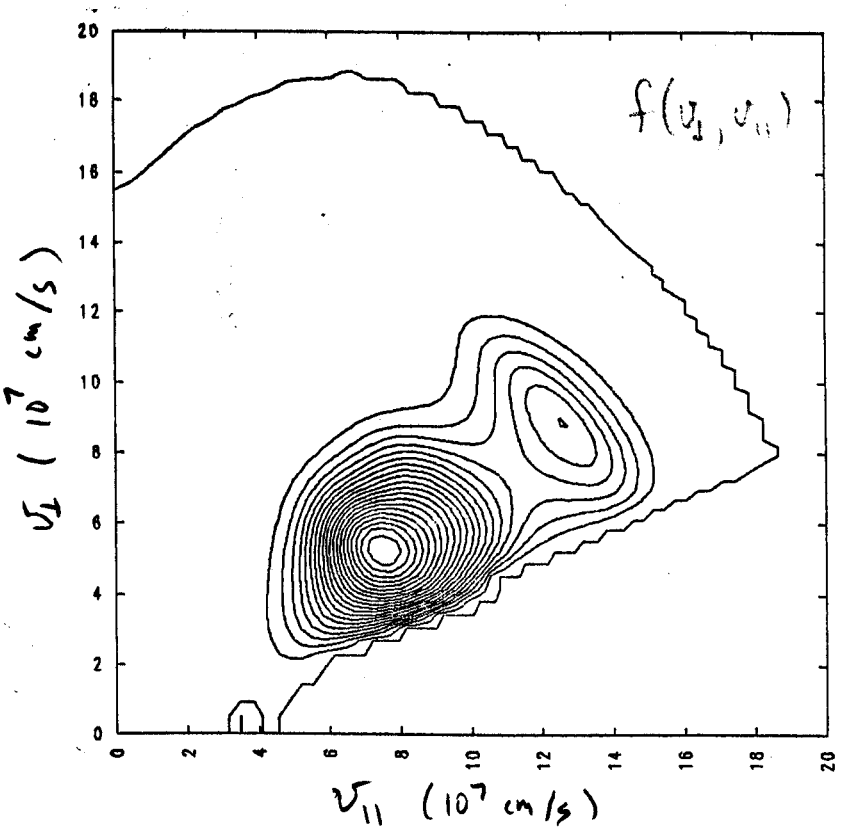

Figure 4: $f(v_{\perp}, v_{||})$ for the ions at the midplane.

FIGURE 5

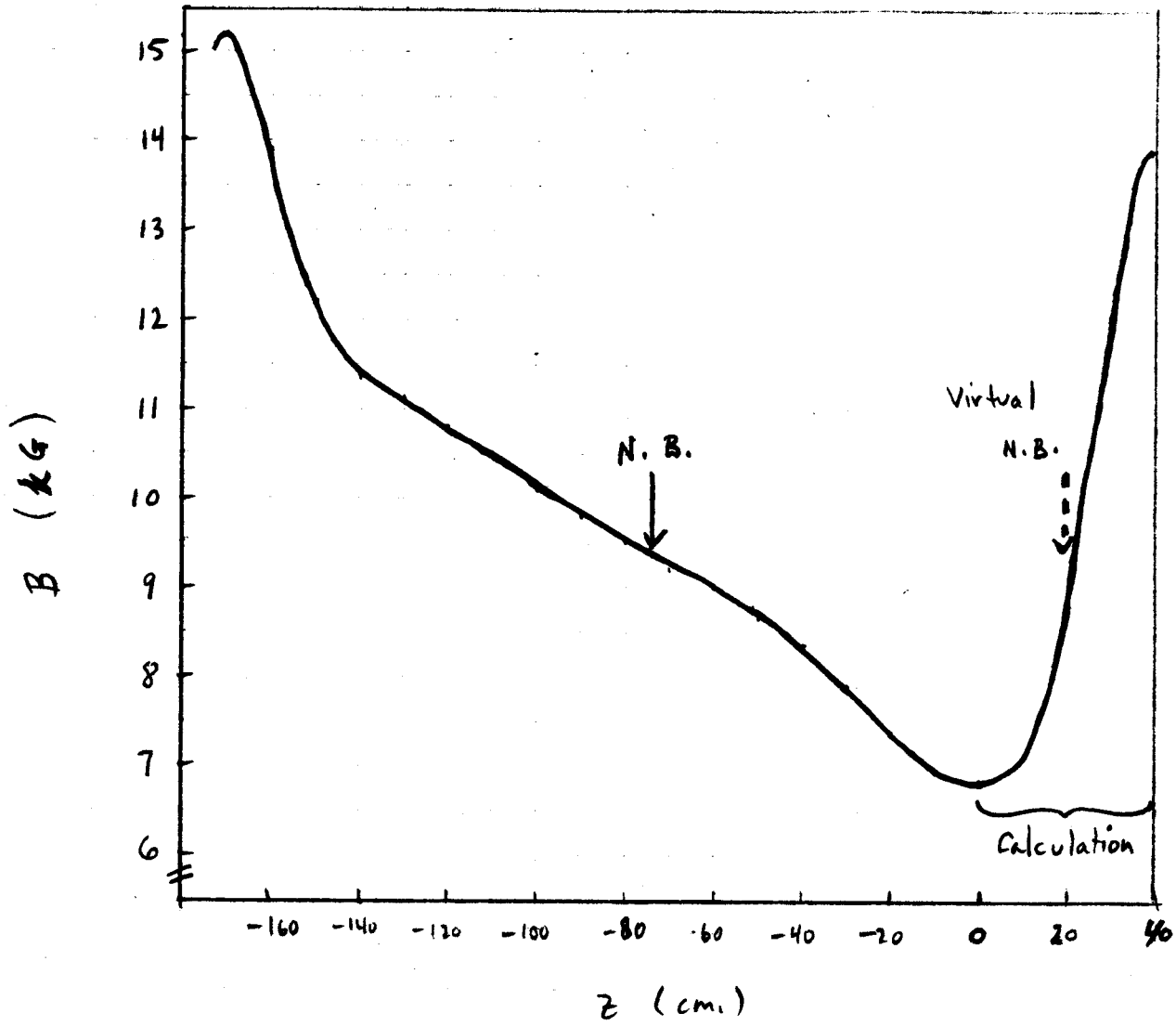

Figure 5: The magnetic field profile for the perpendicular injection case presented in column (b) of table 4. The calculation models the outer part of the mirror indicated by the bracket, and uses a source located at the bounce point of the actual source.

FIGURE 6

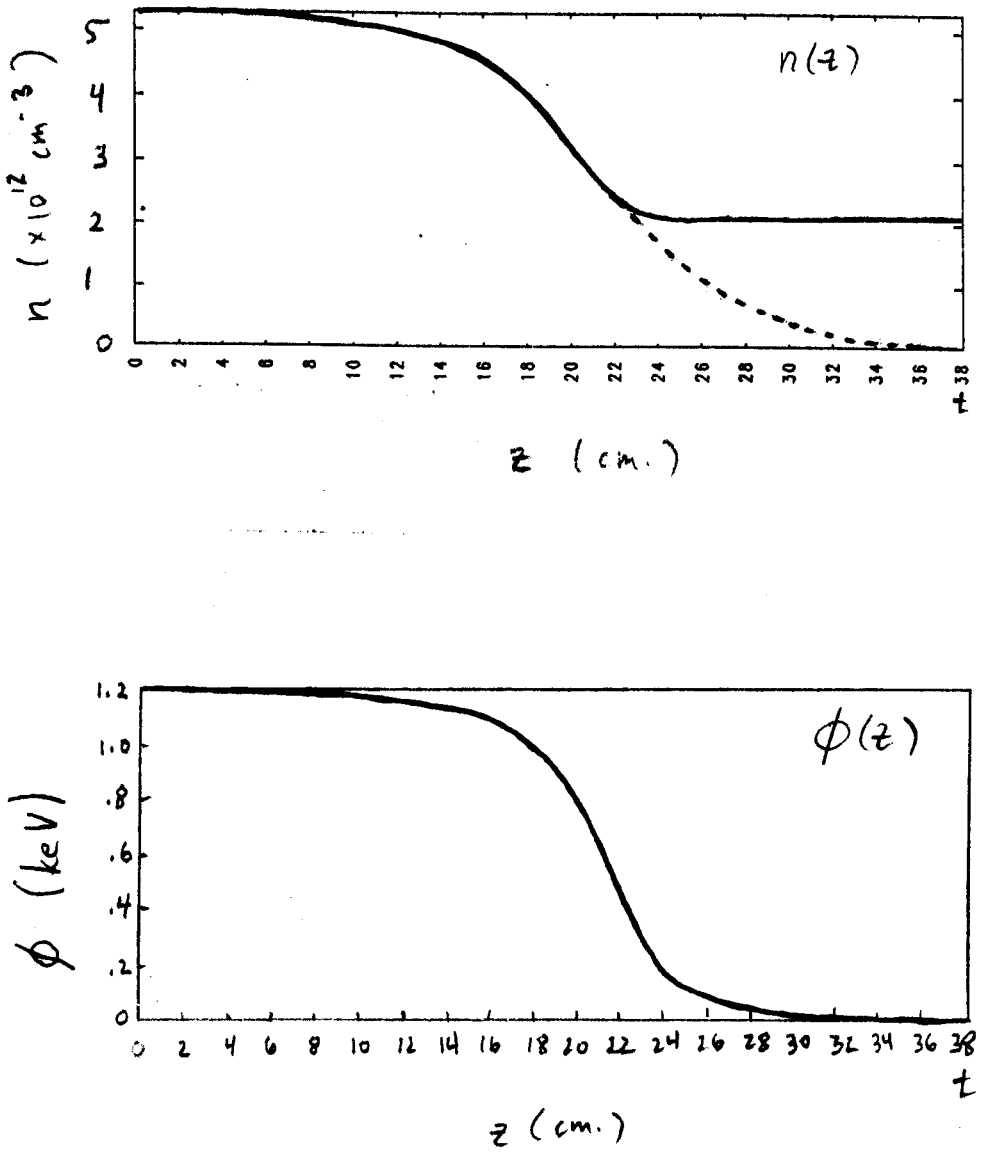

Figure 6: (a) Density profile for the perpendicular injection case. The dotted line indicates the sloshing-ion density, the solid line includes transition density.

(b) The resulting potential profile. Once again the total potential drop is a fixed boundary condition.

FIGURE 7

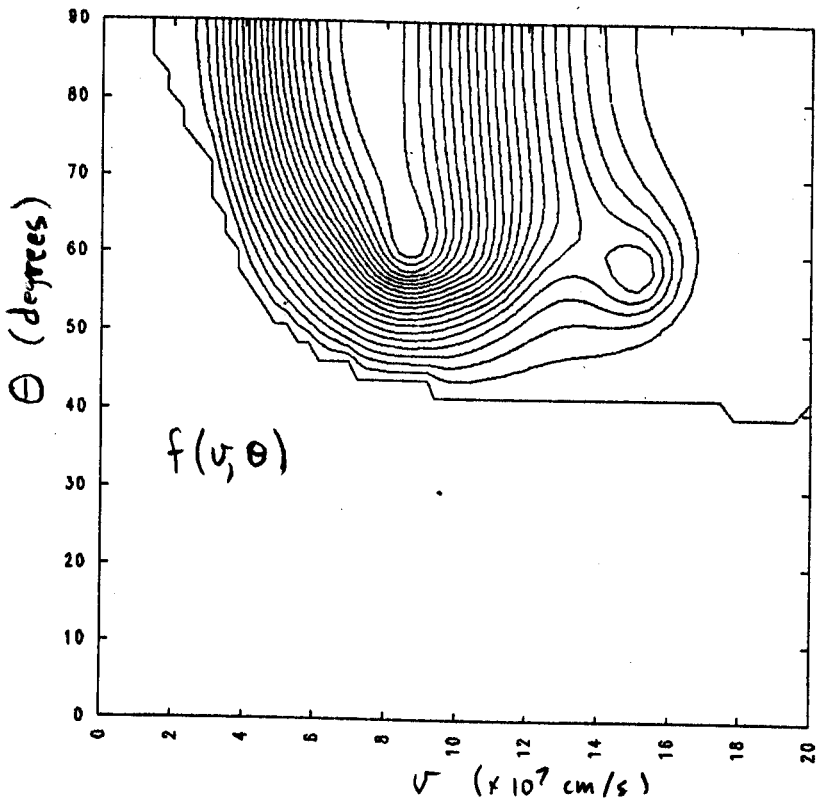

Figure 7: f(v, θ) for the ions at the midplane. Note the considerable spread in pitch angle.

FIGURE 8

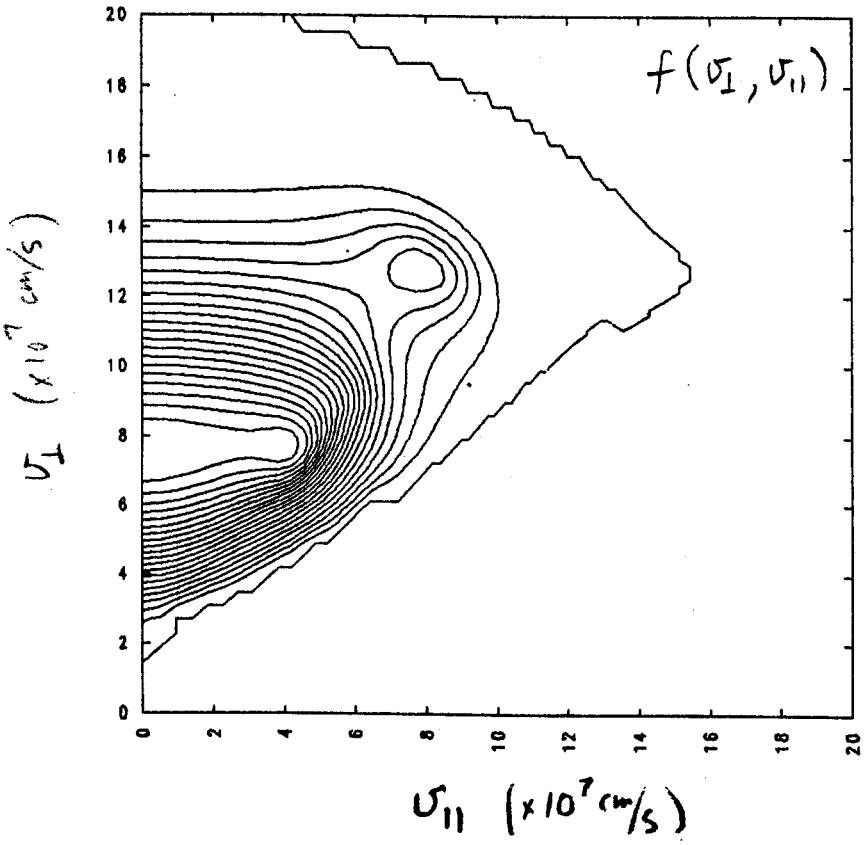

Figure 8: $f(v_\perp, v_{||})$ for the ions at the midplane.